Electronic Supplementary Material (ESI) for Nanoscale.
This journal is © The Royal Society of Chemistry 2014

Supplementary Information:

Quantitative Study of Protein-Protein Interaction by Quartz Nanopipettes

Purushottam Babu Tiwari,[a] Luisana Astudillo,[b] Jaroslava Miksovska,[b] Xuewen Wang,[a] Wenzhi Li,[a]

Yesim Darici,[*a] & Jin He[*a,c]

[a] Department of Physics, Florida International University, Miami, FL 33199

[b] Department of Chemistry and Biochemistry, Florida International University, Miami, FL 33199

[c] Biomolecular Sciences Institute, Florida International University, Miami, FL 33199

[*]Address correspondence to: dariciy@fiu.edu, jinhe@fiu.edu

S1. Determination of nanopipette diameter:

The conical shaped pore geometry of nanopipette is mainly defined by the half cone angle and pore diameter. From the SEM image (Figure S1), we can estimate the average half cone angle of the outer surface to be 1.9^o. Therefore, our estimation for the half cone angle, θ=1.6^o, is reasonable.

If we can ignore the surface charge then the inner diameter of the nanopipette can be derived based on θ and G_p, where G_p is the pore conductance. Referring to the inset of Figure 1d (main text), the IV curves for the bare nanopipettes are always nearly linear and symmetric within the voltage range from -15 mV to +15 mV. The symmetry and linearity of the IV curves suggested that the surface charge effect can be ignored. Therefore, the pore diameter D can be calculated by a simple equation:

$$D = \frac{2G_p}{k}\left[\frac{1}{\pi tan\theta}\right] \qquad \text{Equation (S1)}$$

where κ is the conductivity of electrolyte (25 mM KCl with 2.5 mM PB, pH 7.0).

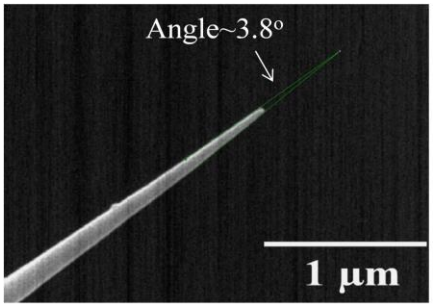

Figure S1: SEM image of a bare pipette tip. The angle is measured by software ImageJ.

S2. Surface modification

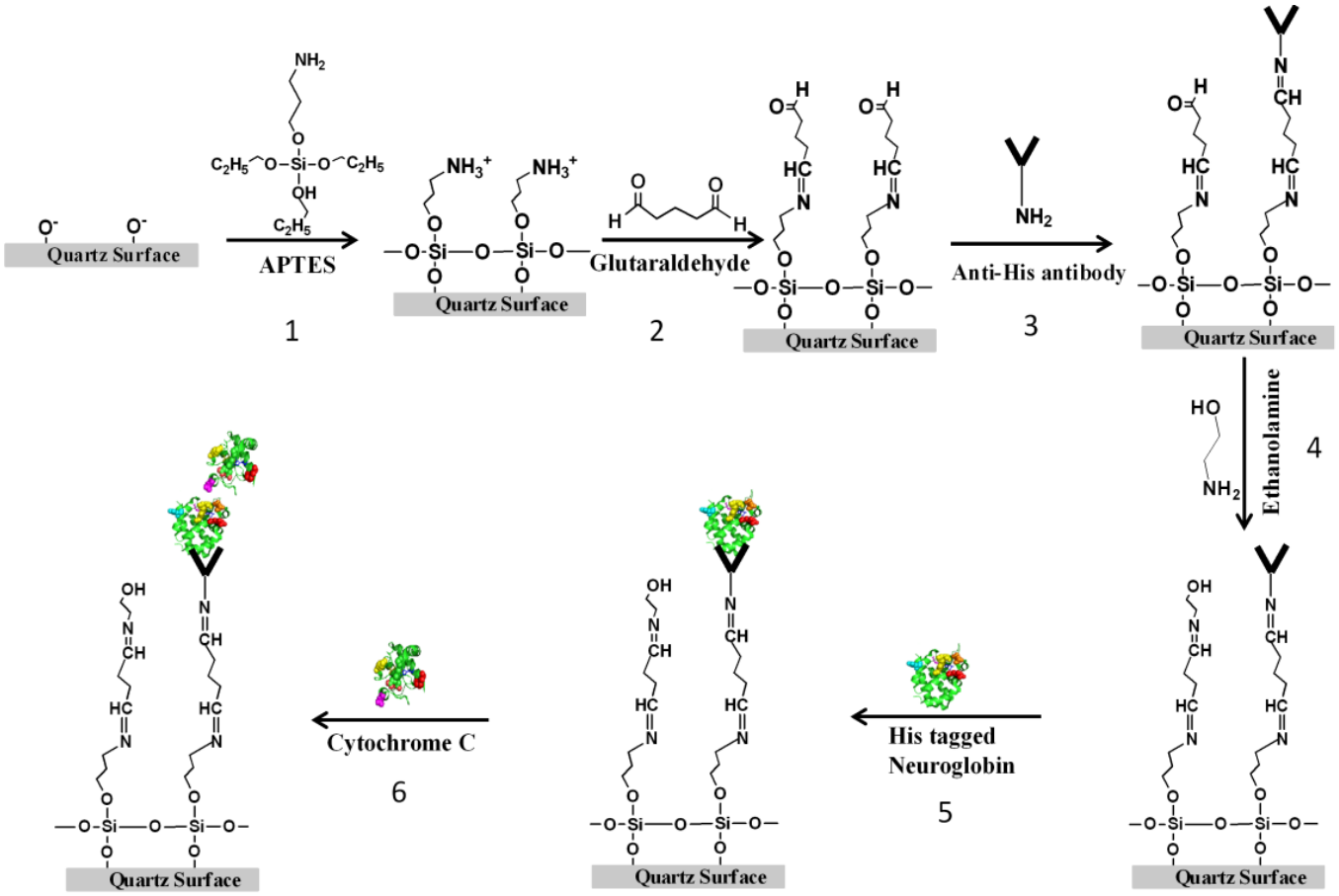

Figure S2. Schematic of the anti-His antibody surface modification method

Before using the anti-His antibody method, we first tested the amide bond method. The nanopipette was sequentially modified with poly-L-lysine (PLL) and polyacrylic acid (PAA) via electrostatic adsorption. Then the Cyt c proteins were immobilized to PAA through the amide bonds by using NHS-EDC coupling chemistry. Based on the rectification ratio r of the modified nanopipettes, 1 out of 4 nanopipettes was modified. However, the measured ionic current was still not stable in our experimental conditions. We also tested the aldehyde-amino chemistry. In this method, the Cyt c proteins were covalently immobilized to the APTES modified nanopipettes through glutaraldehyde. Only 1 out of 6 nanopipettes showed satisfied Cyt c immobilization. Therefore, both methods did not work well as the anti-His antibody method.

S3. Numerical simulation

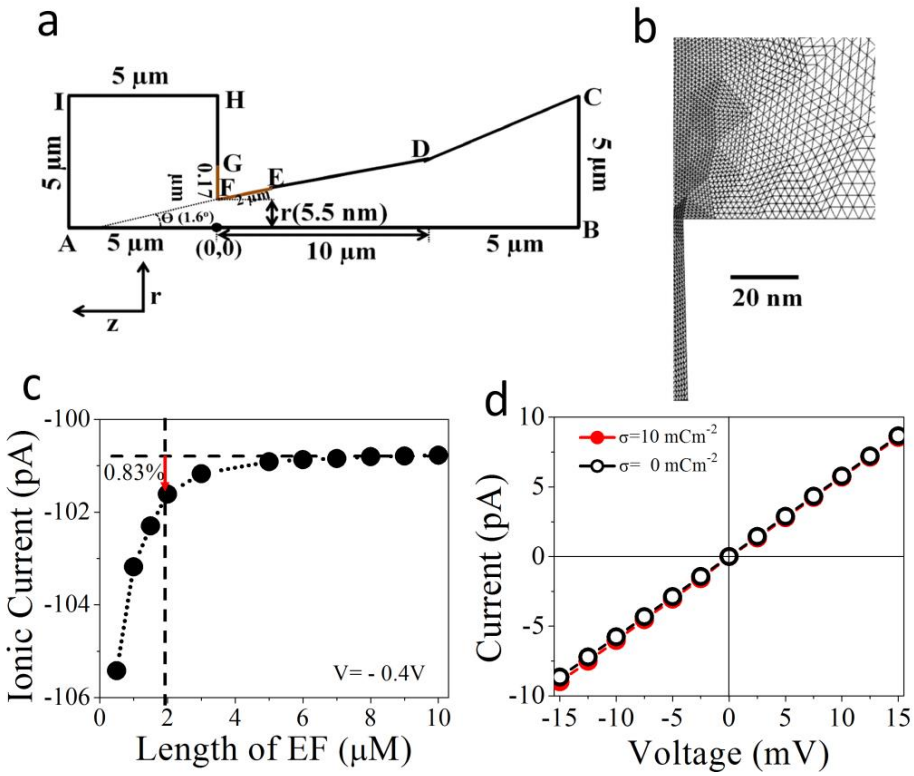

Figure S3: (a) Sketch of the computation domain for the nanopipette. The brown colored EF-FG section has surface charge. The drawing is not to scale. (b) Mesh distribution near the pore mouth. (c) The ionic current at -0.4 V as a function of EF length. (d) Simulated IV curves (within -15 mV- +15 mV bias range) for the pipette with radius 17 nm in the presence and absence of surface charge. The surface charge density σ of EF section is fixed at -4.5 mCm^{-2}. The simulated current magnitude for 2µm EF length is only about 0.83% higher than the one for 10µm EF length. The half cone angle θ was always 1.6°. The change in the surface charge density due to the Cyt c adsorption was estimated using Equation 3 (main text).

Table S1: Boundary selection

Surface	Poisson's equation	Nernst-Plank equation
AB	Axial symmetry	Axial symmetry
BC	Constant electric potential	Constant concentration

CD	Zero charge	No flux (insulation)
DE	Zero charge	No flux (insulation)
EF	Surface charge density	No flux (insulation)
EG	Surface charge density	No flux (insulation)
GH	Zero charge	No flux (insulation)
HI	Zero charge	No flux (insulation)
IA	Ground	Constant concentration

The whole computation domain was discretized into free triangular elements. The following parameters were supplied during simulation;

Parameter	**Value**
Relative permittivity (ε_r)	80
Temperature (T)	298 K
Diffusion coefficient (K^+)	1.957×10^{-9} (m^2s^{-1})
Diffusion coefficient (Cl^-)	2.032×10^{-9} (m^2s^{-1})
Charge number (z_{K+})	1
Charge number (z_{Cl+})	-1
Maximum element (mesh) size	0.8 µm
Maximum element (mesh) size	0.08 nm
Maximum element growth rate	1.4
Resolution of curvature	0.3
Resolution of narrow regions	1
Number of refinements	3

Under the choice of above parameters for EF =2 μm, surface charge density of -4.5 mCm^{-2}, applied potential of -0.4 V, and 5.5 nm pore radius the simulation was finished in 2 minutes 37 seconds.

The following equation was used to calculate ionic current.

$$I = -F \int_S [\boldsymbol{J}(K^+) - \boldsymbol{J}(Cl^-)] \cdot \boldsymbol{n}\, dS \qquad \text{Equation (S2)}$$

As shown in Table S2 below, we compared the rectification ratio r for three different charge distributions. The 2 μm long charged section FE (Figure S3a) is divided into two equal halves. The first half starting from point F is named surface 1 and the second half is named surface 2.

Table S2: Comparison of rectification ratio r

Surface charge density for Surface 1, ρ_1 (mCm^{-2})	Surface charge density for Surface 2, ρ_2 (mCm^{-2})	Average surface charge density $\rho = (\rho_1 + \rho_2)/2$ (mCm^{-2})	Rectification ratio r
-6.5	-2.5	-4.5	-0.38
-2.5	-6.5	-4.5	-0.17
-4.5	-4.5	-4.5	-0.29

S4. Noise analysis

We compared the noise properties of ionic currents recorded for the bare and hNgb modified quartz nanopipettes. The noise power spectrum density (PSD) S(f) can be obtained by performing Fast Fourier Transformations (FFT) of the current time trace (at V = -0.4V) of a nanopore, which were recorded at 250kHz sampling rate with a bandwidth of 100kHz. Figure S4 showed the normalized noise PSDs ($S(f)/\langle I\rangle^2$, where $\langle I\rangle$ is the average current) for the same nanopipette before and after hNgb functionalization. Here we focused on the noise at low frequency regime (f <100 Hz), which is called the 1/f noise or flicker noise. The origin of this noise is still in debate but is assumed to be related to the fluctuations in the charge carrier and surface charge.[1-3] The normalized S(f) in this frequency regime can be fitted by $S(f)/\langle I\rangle^2 = A/f$, where A is the slope of the fitted curve.

As shown in Figure S4, the normalized noise always increases after hNgb modification. The increase of normalized noise can be attributed to the dynamic fluctuation of the modified proteins,

which have been observed in lipid bilayer[4] and Nups proteins[5] modified nanopores. The noise analysis provides additional evidence of the surface modification of the quartz inner surface.

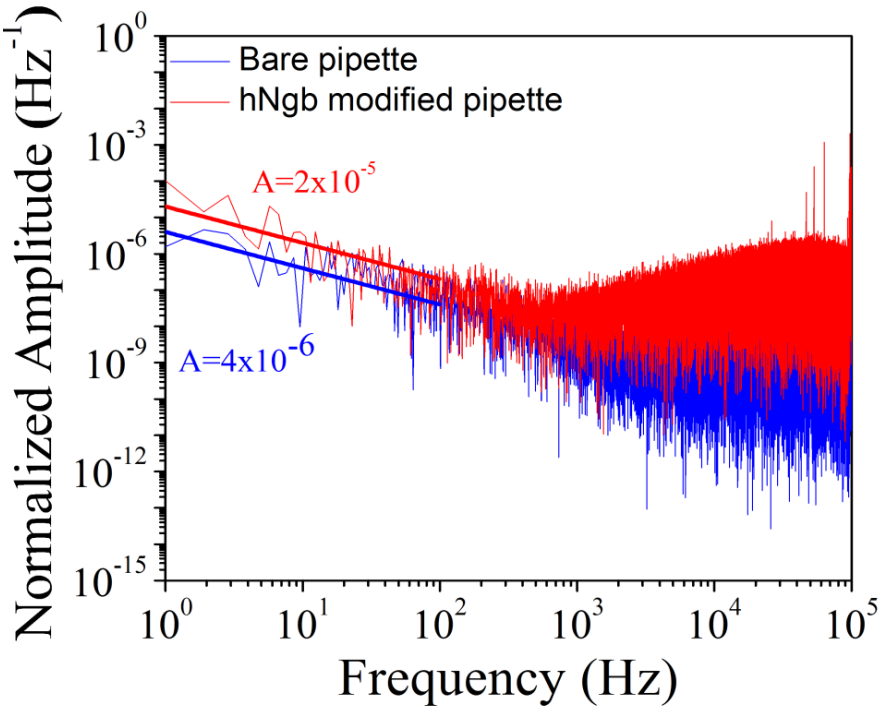

Figure S4. Normalized noise power spectrum for bare pipette (blue) and hNgb modified pipette (red).

S5. Surface Plasmon Resonance (SPR) results

SPR allows real-time and label-free studies of surface chemical modifications and protein-protein interactions. Here we used SPR results to confirm the proposed surface modification steps (section S2) and to obtain the equilibrium dissociation constant K_D of the Cyt c-hNgb interactions.

The SPR system used here is the same as used in previous reports [6, 7] After cleaning with oxygen plasma followed by hydrogen flaming[7], the gold chip was immersed in 5 mM 2-Aminoethanethiol hydrochloride (Acros Organics) in ethanol overnight at 4 ^{o}C to form a self-assembled monolayer (SAM) of cysteamine (CA) on the gold surface, which is analogous to the APTES layer at the quartz pipette surface, with amine terminal groups for aldehyde modification. The modified gold chip was rinsed sequentially using ethanol and DI water, and then dried in Ar flow.

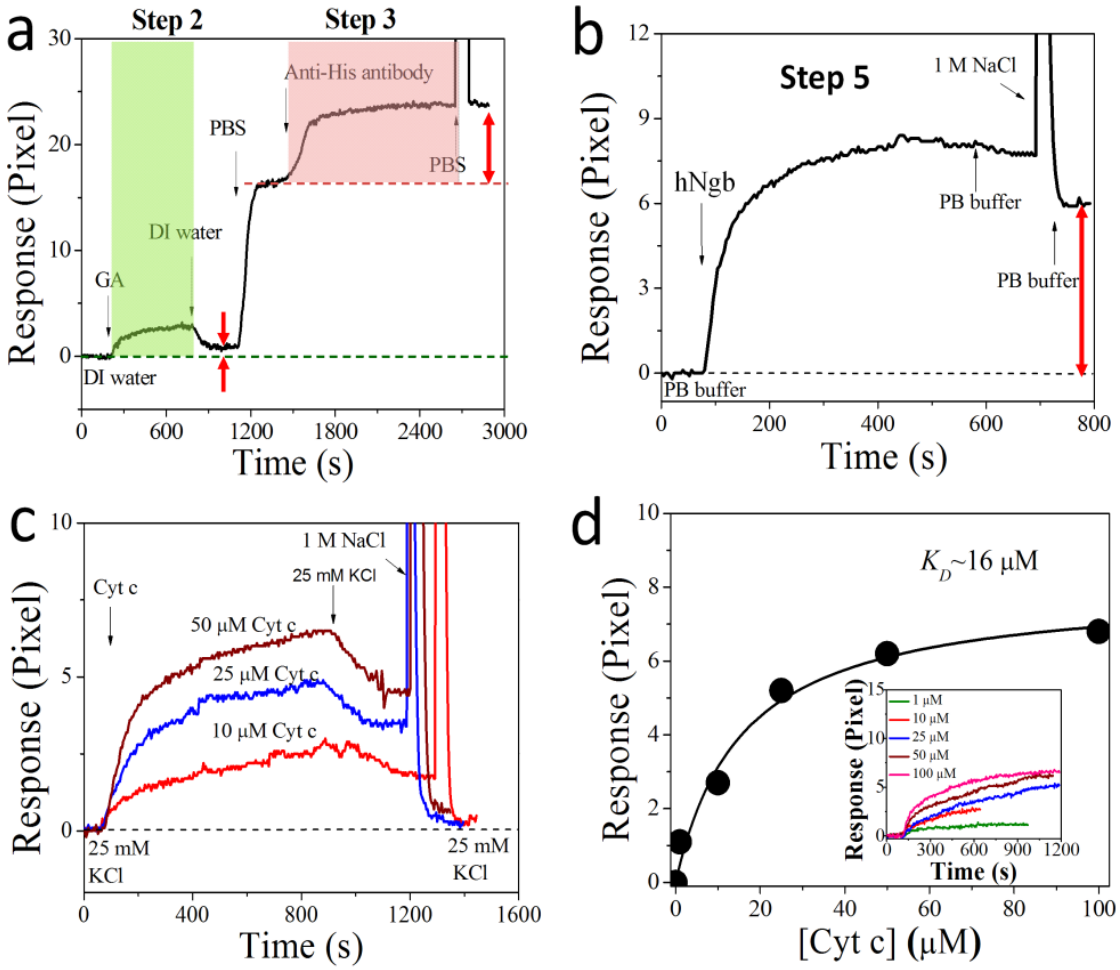

Figure S5: SPR results. (a) Real-time SPR response of the Glutaraldehyde and anti-His antibody modifications. (b) Real-time SPR response of hNgb modification to the anti-His antibody modified surface. (c) SPR response vs. time at different Cyt c concentrations (red color, 10μM; blue color, 25μM; and brown color, 50 μM) showing Cyt c-hNgb complex formation, dissociation, and surface regeneration. The immobilized Cyt c proteins cannot be removed by 25 mM KCl but can be removed by 1 M NaCl. d) SPR response *vs.* Cyt c concentration plot, inset: concentration dependent SPR sensorgrams. The experimental data (solid dots) were fitted (solid line) using Equation S3.

We then used SPR to study the real-time chemical modification of gold surface with cysteamine at a flow rate of 0.05 mL/min. As shown in Figure S5a, the baseline changes after the glutaraldehyde (GA, step 2 of Figure S2) and anti-His antibody (step 3 of Figure S2) modifications,indicate the successful chip surface modification. After the antibody modification, the functionalized chip surface

was treated with 1 M ethanolamine (pH 8.0) to quench excess aldehyde groups. Figure S5b shows the SPR result of the immobilization of His-tagged hNgb onto the antibody surface (step 5 of Figure S2). The hNgb modified surface is quite stable and did not change much even after the flowing of 1 M NaCl solution.

Figure S5c shows the typical SPR results when different concentrations of Cyt c were flowed over the hNgb modified surface. After the quasi equilibrium is reached, 25 mM KCl solution was flowed over the chip surface, which could not break Cyt c-hNgb pairs. However, the flow of 1 M NaCl solution could successfully remove Cyt c from the surface, and hNgb surface was regenerated. We determined the K_D for the Cyt c -hNgb interactions using equilibrium analysis method. Figure S5d shows the SPR response vs. Cyt c concentrations. The following equation is used to fit the experimental data,

$$R = \frac{R_{\max}[A]}{K_d + [A]} \qquad \text{Equation (S3)}$$

where R is the SPR equilibrium response, R_{max} is fitting parameter representing maximum response, and [A] is the analyte (Cyt c) concentration. We obtained K_D value of ~16 μM for the Cyt c-hNgb interactions.

S6: Lysozyme control experiment using SPR

Control experiments were carried out by SPR to study the interactions between Lysozyme (Lsz) and hNgb. As shown in the sensorgrams of Figure S6, the Lsz-hNgb complex is highly dissociable. After treated with 25mM KCl, there is a large decrease of the response signal, and the response signals lost protein concentration dependence (as indicated by red arrow). In contrast, the Cyt c-hNgb complex is stable during 25mM KCl flowing thereby showing much smaller decrease in response signal magnitude (Figure S5c).

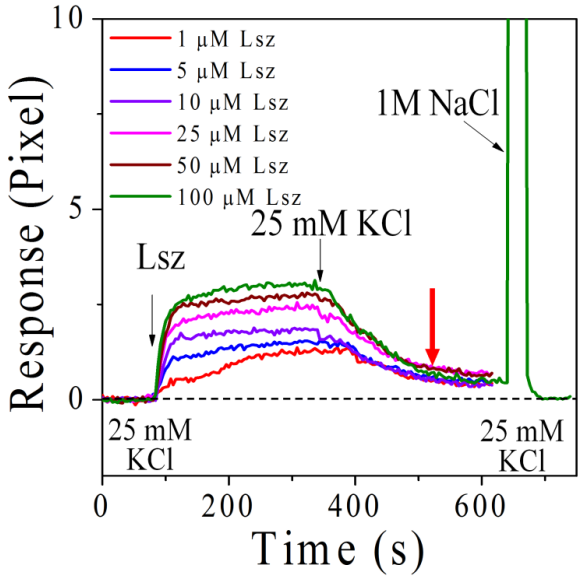

Figure S6: SPR sensorgrams for Lsz binding to hNgb.

S7: Titration curves for Cyt c-hNgb interactions as determined by numerical simulations

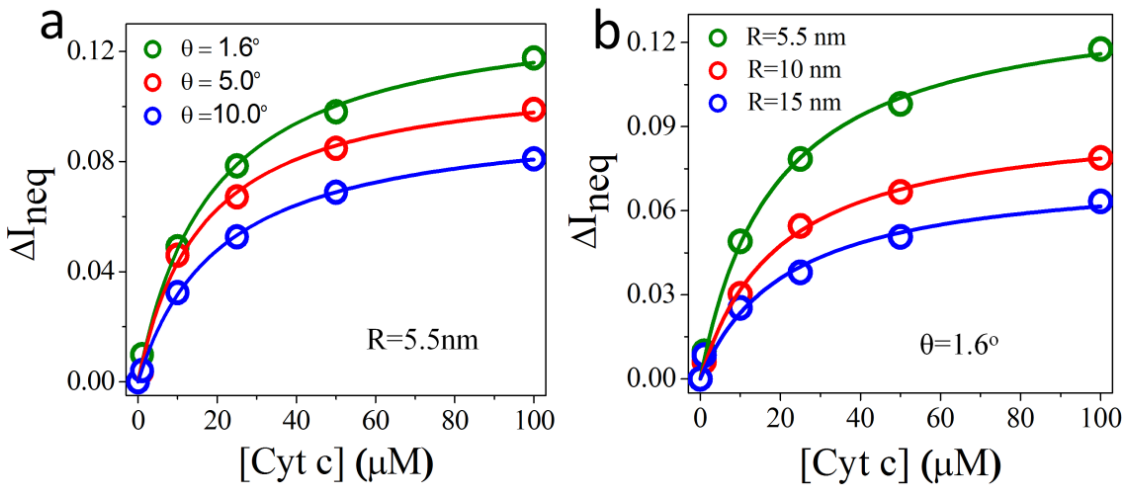

Figure S7: (a) Simulated ΔI_{neq}-[Cyt c] plots at different half cone angles. The pipette radius R was always 5.5 nm. (b) Simulated ΔI_{neq}-[Cyt c] plots at different pore radius. The initial surface charge density was -4.5 mCm^{-2}. All the simulated data (open dots) can be fitted (solid lines) using Equation 1 with K_D=20 µM.

References

1. P. Chen, T. Mitsui, D. B. Farmer, J. Golovchenko, R. G. Gordon and D. Branton, *Nano. Lett.*, 2004, **4**, 1333-1337.
2. R. M. M. Smeets, U. F. Keyser, N. H. Dekker and C. Dekker, *Proc. Natl. Acad. Sci.*, 2008, **105**, 417-421.
3. D. P. Hoogerheide, S. Garaj and J. A. Golovchenko, *Phys. Rev. Lett.*, 2009, **102**, 256804.
4. E. C. Yusko, J. M. Johnson, S. Majd, P. Prangkio, R. C. Rollings, J. Li, J. Yang and M. Mayer, *Nat. Nanotechnol.*, 2011, **6**, 253-260.
5. S. W. Kowalczyk, L. Kapinos, T. R. Blosser, T. Magalhaes, P. van Nies, Y. H. LimRoderick and C. Dekker, *Nat. Nanotechnol.*, 2011, **6**, 433-438.
6. N. M. Mulchan, M. Rodriguez, K. O'Shea and Y. Darici, *Sens. Actuat. B-Chem.*, 2003, **88**, 132-137.
7. P. B. Tiwari, T. Annamalai, B. Cheng, G. Narula, X. Wang, Y.-C. Tse-Dinh, J. He and Y. Darici, *Biochem. Biophys. Res. Commun.*, 2014, **445**, 445-450.